Effect of Droplet-Removal Processes on Fog-Harvesting Performance on Wettability-Controlled Wire Array with Staggered Arrangement

Yutaka Yamada†*, *Junya Oka*‡, *Kazuma Isobe*†, *and Akihiko Horibe*†

†Faculty of Environmental, Life, Natural Science and Technology, Okayama University, 3-1-1 Tsushima-naka, Kita-ku, Okayama 700-8530, Japan

‡Graduate School of Natural Science and Technology, Okayama University, 3-1-1 Tsushima-naka, Kita-ku, Okayama 700-8530, Japan

*Corresponding Author

Yutaka Yamada

Tel.: +81 86 251 8046; E-mail: y.yamada@okayama-u.ac.jp

ABSTRACT

Development of freshwater resources is vital to overcome severe worldwide water scarcity. Fog harvesting has attracted attention as a candidate technology that can be used to obtain fresh water from a foggy air stream without energy input. Drainage of captured droplets from fog harvesters is necessary to maintain permeability of harp-shaped harvesters. In the present study, we investigated the effect of droplet-removal process on the amount of water harvested using a harvester constructed by wettability-controlled wires with an alternating and staggered arrangement. Droplet transfer from hydrophobic to hydrophilic wires, located upstream and downstream of the fog flow, respectively, was observed with a fog velocity higher than 1.5 m/s. The proportion of harvesting resulting from droplet transfer exceeded 30% of the total and it reflected more than 20% increase of the harvesting performance compared with that of a harvester with wires of the same wettability: this value varied with the adhesive property of the wires and fog velocity. Scaled-up and multilayered harvesters were developed to enhance the harvesting performance. We demonstrated certain enhancements under multilayered conditions and obtained 15.99 g/30 min as the maximum harvested amount, which corresponds to 13.3% of the liquid contained in the fog stream and enhances by 10% compared with that without droplet transfer.

INTRODUCTION

Fresh water, which is a necessary resource for agricultural, industrial, and daily use, is facing worldwide scarcity due to population growth, economic development, and changing consumption patterns.[1, 2] In particular, four billion people suffer water scarcity for at least one month of the year.[2] Nevertheless, water demand has increased over the past 40 years and continuous growth is expected until 2050,[1] which exacerbates this situation. Techniques such as desalination, reverse osmosis, cloud seeding, dew condensation, fog harvesting, and sorbent-based atmospheric water harvesting are expected to serve important roles in providing fresh water;[3–10] however, concerns, such as energy input, location limitation, and environmental impact, have been raised for the first three technologies listed above.[3,4] The latter three methods obtain fresh water from vapor or tiny droplets in the air. Although these latter methods overcome some of the abovementioned drawbacks, some energy input is still required to obtain liquid from vapor. Given these considerations, fog harvesting has attracted significant attention as a low-cost and low-energy consumption technology.[7,11,12]

The principle of fog harvesting lies in the collision of tiny droplets with a solid object and already attached liquid, with subsequent drainage of the accumulated water from a harvester. The former process mainly depends on aerodynamic and deposition efficiencies, which are a function of fog velocity, size and shape of the solid object, and other factors.[12,13] The latter involves transportation of the attached droplets. Because droplets attached to a harvester are unusable for other purposes, these droplets should be transferred and stored in a reserver tank; thus, mechanisms to initiate droplet transfer serve an important role. Use of a wettability gradient and Laplace pressure

difference in the droplet have attracted significant attention.[14,15] These processes are inspired by insects,[16,17], plants,[18,19] and animals,[20] and are emulated using several complicated fabrication techniques.[21–26] For example, Ju et al.[26] fabricated a conical copper wire by electrochemical corrosion and then modified the wettability to be hydrophobic at its tip and hydrophilic at its root. Because both gradient characteristics contribute to drive droplets from the tip to the root, efficient droplet transfer was achieved. Although these biomimetic approaches enhance fog-harvesting performance, complicated fabrication techniques are not suitable or have to overcome significant difficulties in scale-up of the fog harvester.

A surface-type material is a strong candidate for a scalable fog harvester.[27,28] Biomimetic approaches are helpful in initiating droplet motion and have been used in many investigations.[29–32] For example, Bai et al.[29] and Kostal et al.[30] fabricated patterned wettability surfaces and showed an enhancement in the amount of fog harvested compared with that of uniform wettability surfaces. However, considering enhancement of the harvested amount, surface-type harvesters showed poorer performance than permeable harvesters, such as the mesh and harp types.[31,33] This is due to the decrease in fog velocity in the vicinity of the harvester due to blockage of the fog stream.[33] In addition, the blockage increases the aerodynamic force, which affects the harvester and should be avoided to prevent damage to the structure. Accordingly, mesh and harp structures have been widely investigated, although they suffer from drainage problems, in particular, clogging of mesh structures and tangling in harp structures.[33–37] Clogging of the mesh pore disturbs the fog flow through the

pores and depresses harvesting efficiency.[33] Tangling is the deformation behavior of a harp structure caused by the capillary force acting on elastic wires.[37–39] This partially induces large gaps in the harp structure, which degrades harvesting performance.[37] To overcome these issues, a mechanism to initiate droplet motion along the fog stream has been considered, instead of relying on drainage by the gravitational force. Typical examples are the Janus mesh and Janus membrane,[40–42] which have a hydrophobic feature facing the fog stream and a hydrophilic feature at the opposite side. However, tiny pores are still subject to clogging,[41] so large pores are required to maintain permeability.[33,41] This reduces the shade coefficient and affects to the fog-harvesting efficiency.[43–45]

In the present study, we prepared a harp-type fog harvester constructed using hydrophobic and hydrophilic wires that are alternately aligned in a staggered arrangement.[46] Unidirectional droplet transfer from the hydrophobic wire to hydrophilic wire was observed at a fog velocity above 1.5 m/s; roll off due to the gravitational force dominated at lower velocity. We analyzed the contribution of the droplet-transfer process to the harvested amount and found that more than 30% of the collected water was drained by this process. In addition, we investigated the fog-harvesting performance of a scaled-up, multilayered harvester: this collected 13.3% of the liquid contained in a fog stream.

EXPERIMENTAL METHODS

Materials

Copper wires with diameter of 0.5 mm were used as the initial material for the fog harvester. Ethanol and hydrochloric acid (HCl) were acquired from Fujifilm Wako Pure Chemical Co. (Japan) and used as solvents. Ammonium persulfate ($(NH_4)_2S_2O_8$), sodium hydroxide (NaOH), and sodium hydrogen carbonate ($NaHCO_3$) (Fujifilm Wako Pure Chemical Co.) were used for the fabrication of nanostructures on the wire surfaces. 6-Mercapto-1-hexanol (Sigma-Aldrich, USA) and Teflon AF 1600X (Mitsui-DuPont Fluorochemical Co., Japan) were used as wettability modifiers. FC-770 (Hayashi Pure Chemical Industry Ltd., Japan) was used as a solvent for wettability modification. Owing to the difficulty of undertaking wettability measurements on a single wire, copper substrates with size of 10 mm × 10 mm were prepared.

Sample preparation and characterization

Wires with four different wettability characteristics; namely, superhydrophilic (SHL), hydrophobic (HB), superhydrophobic (SHB), and adhesive petal (P), were prepared by following procedures provided elsewhere.[46] Brief details of the preparation procedure are provided here. After adjusting the length of the copper wires to 65 mm, they were cleaned in ethanol by ultrasonication for 15 min and then rinsed with purified water (CPW-102, Advantec Co., Japan). Except for preparation of the HB wires, the native oxide layer on the wire was removed by immersion in 6 M HCl aqueous solution for 20 s. To fabricate the nanostructures on the SHL and SHB wires, the wires were dipped into an aqueous solution of 2.5 M NaOH and 0.1 M $(NH_4)_2S_2O_8$ for 20 min at 4°C. After rinsing with purified water and dried by a compressed air flow, the wires were heated at 180°C for 2

h to dehydrate the structure. For wire P, the structure was fabricated by immersing the copper wires in an aqueous solution of 0.1 M $NaHCO_3$ and 0.02 M $(NH_4)_2S_2O_8$ for 24 h at 20–25°C, then rinsed with purified water and dried. Wettability modifications were conducted as follows. The SHL wires were dipped in 10 mM 6-mercapto-1-hexanol solution in ethanol for 5 min, then rinsed with ethanol and water to removed unreacted materials. The other three wire types were dipped in FC-770 solution with 0.5 mass% Teflon AF 1600X for 30 s to provide a hydrophobic coating and then heated at 90°C for 60 min.

Fabricated nanostructures on the wire surfaces were analyzed by scanning electron microscope (SEM; JEOL7001F, JEOL Co., Japan). Figure 1 shows SEM images of the surface structures of the wires prepared by each procedure. Because the surface structures were formed by chemical etching while the wettability modification processes had no effect on the form of the structure, the structures on the SHL and SHB surfaces were basically equivalent and are shown as Figure 1(a). Randomly oriented needle-like structures with a diameter of less than 1 μm was observed

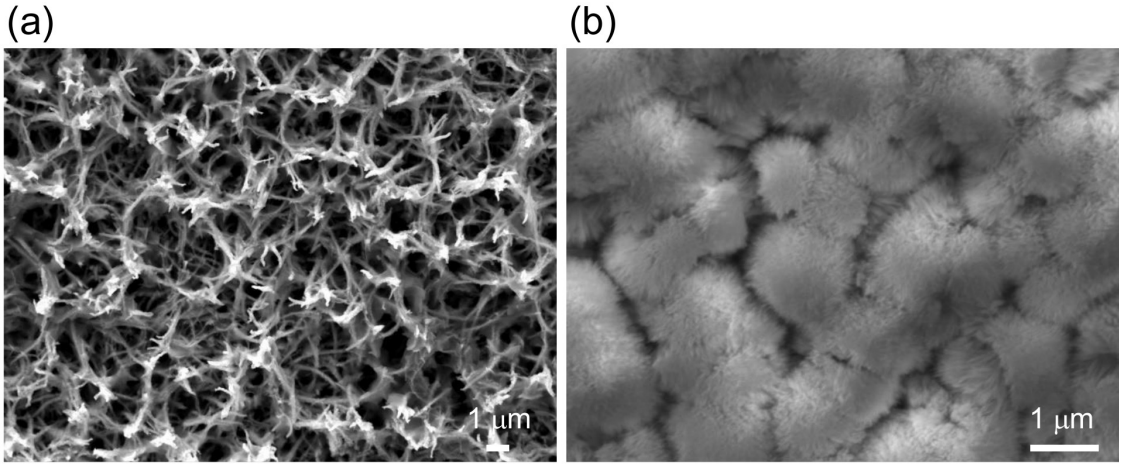

Figure 1 SEM observation result of (a) SHB and SHL surface and (b) P surface.

on the surface. For the P surface, further small needle-like structures were observed on the spherical bump structures.

Because the droplet size required for wettability characterization is large compared with the wire diameter, flat copper surfaces treated by same procedures were prepared and used for characterization. The sessile droplet method was used to characterize the static contact angle. Advancing and receding contact angles were acquired by three-phase contact-line motion during increasing and decreasing the volume of a droplet placed on the surface. As previously reported,[46] the static contact angle of the SHL surface was < 3°; dynamic contact angles were unmeasurable because its superhydrophilicity. The HB, SHB, and P surfaces showed 118°, 156°, and 154° as static contact angles, while the advancing and receding angles were 122° and 110° for HB, 160° and 154° for SHB, and 161° and 107° for the P surfaces, respectively. The contact angle hysteresis, defined as the difference between the advancing and receding angles, was 6° for the SHB surface, but 54° for the P surface, confirming that the P surface had more adhesive features.

Fog-harvesting experiments

Figure 2(a) shows the experimental setup for the fog-harvesting experiments. Fog was generated by a fog generator (IM4-36D/S, Seiko Giken, Japan) and ejected by a throat with a cross-sectional area of 25 mm × 25 mm. A fog-harvesting unit was placed on a plastic dish to collect drained liquid and located 40 mm downstream of the exit of the fog stream. This consisted of wires prepared as described in the sample preparation section; detail of the configuration is shown in Figure 2(b).

The values of the interval w and depth d of the wire locations were chosen to be 2.0 and 1.0 mm, respectively, and the wire on the downstream side was located midway between the two wires located on the upstream side because this configuration showed the maximum harvested amount.[46] Both ends of these wires were fixed to a frame with 70 mm height, 62 mm width, and a thickness of 10 mm. Details of the wire arrangements for each unit are summarized in Table 1. Unit 1 (U1) consisted of HB wires only because the amount of fog harvested by a single HB wire was larger than other three types, as previously reported.[46] Units 2 and 3 (U2 and U3) had SHB or P wires at the upstream side, respectively, and SHL wires at downstream side. This wettability difference induced droplet transfer when droplets attached to wires on the upstream side reached the SHL wire. In addition, two further types of experiments were conducted: one used units with three wires (two upstream and one

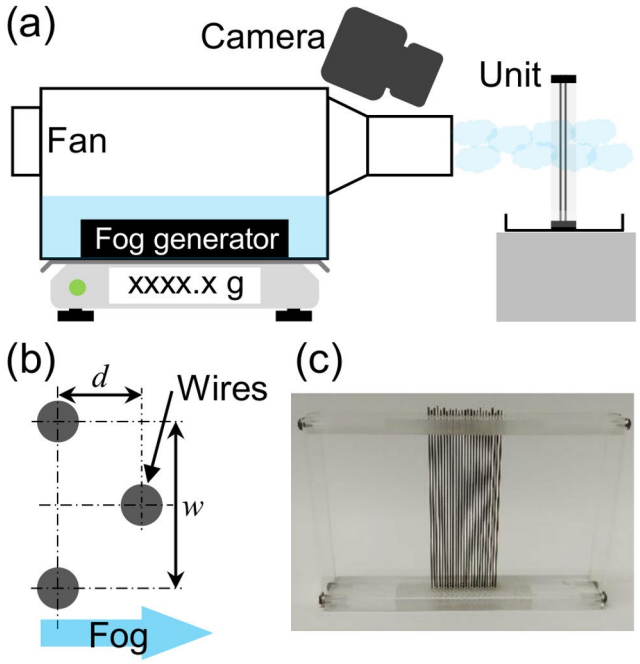

Figure 2(a) Schematic of experimental setup for fog-harvesting experiments. (b) Top view of three-wire configuration of fog-harvesting unit. (c) Photograph of a scaled-up fog harvester.

Table 1 Wettability patterns for fog-harvesting experiments

Unit name	Upstream side	Downstream side
U1	HB	HB
U2	SHB	SHL
U3	P	SHL

downstream) to investigate the relation between the harvested amount and droplet-removal processes; the other was a scaled-up experiment with a unit constructed of 25 wires (13 upstream and 12 downstream), as shown in Figure 2(c). The shade coefficient *SC* which corresponds to the solid fraction facing normal to the fog flow[12] of this configuration is 0.5. This unit was stacked in three layers along the direction of fog flow. In this case, the distance between wires on the downstream side of front layer and those on the upstream side of rear layer was set at 1 mm.

All fog-harvesting experiments were conducted under fog streams of 1.0, 1.5, and 2.0 m/s with a water content of 240 ± 8 g/h. Ambient temperature and relative humidity were 20.5 ± 1.0°C and 65 ± 10%, respectively. The measurements at each condition were conducted three times and the duration of each trial was 30 min. The amount of harvested water, which included both liquid drained from the wires and droplets remaining on the wires, was measured by an electric balance after each experiment. In addition, behavior of the droplet-removal process was recorded by a camera (D5300, Nikon, Japan) and significant change of the removal process was not observed during our experiments.

RESULTS AND DISCUSSION

The three prepared wires were arranged following the patterns shown in Table 1 to investigate the effect of droplet-transfer process on the amount of fog harvested. The plots shown in Figure 3 indicate the experimental results for each unit and the associated scatter bars represent the variation in measured values for different experimental runs. As a general trend, the amount of fog harvested increased with increase in the fog velocity; however, this increase significantly diminished with further increase in the fog velocity due to detachment of the droplets. Comparing the same fog velocity, U2 and U3 collected larger amounts of water than U1 because the observed droplet-removal processes varied with the wire arrangement.

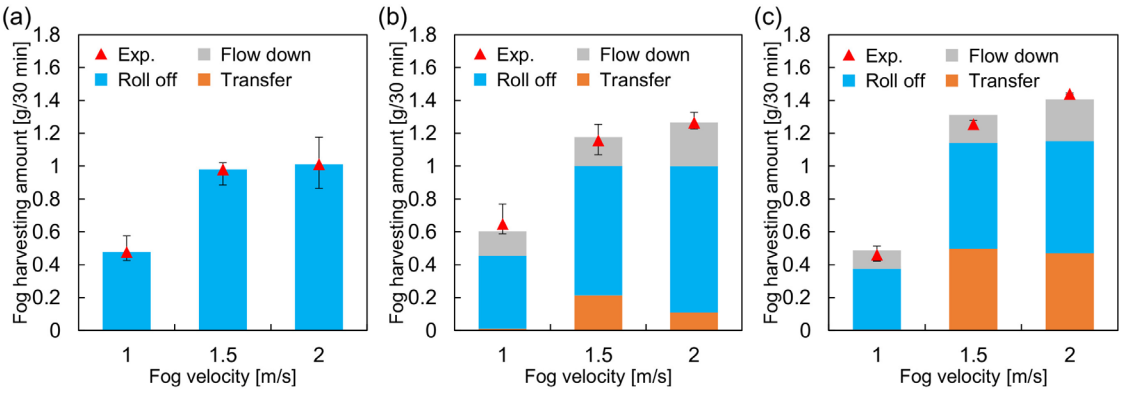

Figure 3 Amounts of fog harvested using three-wire configurations: (a) U1, (b) U2, and (c) U3.

Three types of droplet-removal processes were observed, the schematics of which are shown in Figure 4. Figure 4(a) shows flow of the droplet down the SHL wire: oval-shaped droplets continuously flowed down on a liquid film attached to the SHL wire. Figure 4(b) shows the roll-off behavior of droplets (see Video S1) that could be seen on the HB, SHB, and P wires. Here, attached

droplets rolled off by gravitational and/or aerodynamic forces due to the fog stream. During this behavior, droplets attached to the bottom of the same wire got caught in the rolled-off droplet and a droplet-free surface was exposed. Accordingly, the actual shade coefficient, which is affected by the morphology of attached droplets, was significantly decreased and suppressed the efficiency of fog-droplet collection. Figure 4(c) shows droplet transfer from upstream to downstream wires and Fig. 4(d) shows sequential images during this process (see Video S2). In detail, droplets attached to the SHB and P wires moved along the fog flow direction by the acting aerodynamic force. When a droplet was large enough to reach the SHL wire located downstream side, the droplet transferred to the SHL

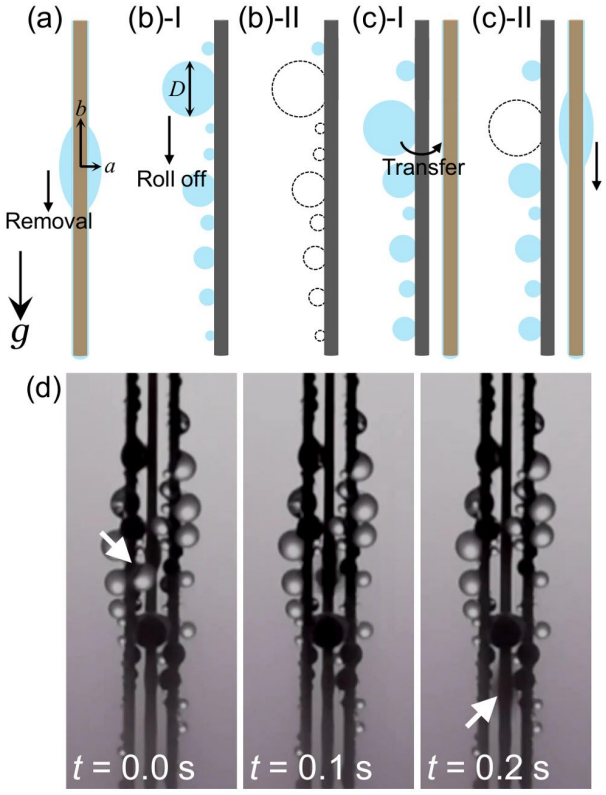

Figure 4 Schematics of droplet-removal processes from fog-harvesting wires (at side view): (a) flow down from SHL wire, (b) roll off from HB, SHB, and P wires, and (c) transfer from SHB and P to SHL wires. (d) Snapshot images during droplet transfer process.

wire as shown the droplet indicated by arrow in Fig. 4(d), while other droplets attached to the bottom of the same wire remained. This behavior was observed for U2 and U3, which gave higher harvested amounts than U1.

To analyze the relationship between the droplet-removal processes and the harvested amount, we estimated a volume of each droplet removed according to the droplet shape. As shown in Figure 4(a), a minor radius a and major radius b of each oval-shaped droplet was measured and the volume was estimated by the following equation:

$$V_{\mathrm{a}} = \frac{4}{3}\pi a^2 b - 2\pi b r^2, \tag{1}$$

where r is the radius of the wire. For spherical droplets, shown in Figure 4(b) and (c), the diameter of each droplet was used to estimate the volume as follows:

$$V_{\mathrm{b}} = \frac{\pi h}{6}\left(3c^2 + h^2\right), \tag{2}$$

where the contact radius c and droplet height h are associated with the diameter D as $c = \frac{D}{2}\cos\left(\theta - \frac{\pi}{2}\right)$ and $h = \frac{D}{2} + \frac{D}{2}\sin\left(\theta - \frac{\pi}{2}\right)$, respectively. Here, θ is the contact angle of the droplet, which was estimated from the results obtained for the respective flat surfaces, i.e., the effect of surface curvature was ignored in this droplet volume estimation.

Using Equations 1 and 2, and the videos of the experiments, we estimated the amount of fog harvested by each droplet-removal process. The results are shown as the colored bars in Figure 3. Here, the removal process of several droplets changed from roll off to transfer before the droplets completely rolled off: these are counted as droplet transfer. The estimated total harvested amounts

are comparable with the experimental results. This indicates that the present estimation method appropriately evaluates the droplet volume for each removal process.

Focusing on the difference between the droplet-removal processes, the amount harvested from U1, shown in Figure 3(a), occurred only by the droplet roll-off process, regardless of the fog velocity, because the SHL wire (which involves flow down and transfer processes) was absent. For U2 and U3, all removal processes appeared, as shown in Figures 3(b) and (c); however, droplet transfer was absent at a fog velocity of 1.0 m/s because the fog stream was insufficient to initiate droplet motion on the wires. This result suggests the applicable limitation of the droplet-transfer mechanism. At 1.5 m/s, the proportion of the transfer process relative to the total harvested amount increased to 18% and 38% for U2 and U3, respectively, which indicated that the contribution by the roll-off process decreased. Differences between the units was caused by the dynamic wettability of the wire surfaces: as shown in Table 1, the wettability of wires located on the upstream side of U2 were superhydrophobic, while those of U3 had high adhesion. The force required for motion of the three-phase contact line f can be shown as:

$$f \approx \gamma_{\mathrm{LV}}\left(\cos\theta_{\mathrm{r}} - \cos\theta_{\mathrm{a}}\right), \tag{3}$$

where γ_{LV} is the surface tension between the liquid and gas phases, θ_{r} and θ_{a} are the receding and advancing contact angles, respectively. In general, a small difference between these angles needs a small force to initiate motion of the droplet, so droplets on SHB wires need less force. However, in the present case, this low threshold induced motion of droplets with insufficient size to reach the SHL

wire. These droplets were detached from the wire by the fog stream or merged with other droplets on the same wire to initiate the roll-off process. In contrast, droplets on P wires required a further large aerodynamic force to initiate motion; therefore, sufficiently large droplets only moved after growth on the wires. The decrease in the proportion of droplet transfer at 2.0 m/s on U2, shown in Figure 3(b), can be considered as an increase in droplet motion with further smaller size. Although there is a trade-off between the roll-off and transfer processes, the amount harvested by the flow-down process increased with increase of the fog velocity. This is attributed to the fog droplet deposition efficiency η_d, which is expressed as follows:[12]

$$\eta_d = \frac{St}{St + \pi/2}, \tag{4}$$

and depends on the fog velocity. This can be associated with the Stokes number *St*, which is defined by the following equation:

$$St = \frac{2\rho_{water} v R_{fog}^{\ 2}}{9\mu_{air} r}, \tag{5}$$

where ρ_{water} is the density of water, v is the velocity of the fog stream, R_{fog} is the radius of the fog droplets, and μ_{air} is the viscosity of air. *St* is an index used to evaluate particle motion around an obstacle: a value larger than unity suggests that motion of the particle will not follow the streamlines around the obstacle. Hence, fog droplets with larger velocity were captured by harvester and, as a result, the amount harvested by the flow-down process increased.

As shown above, the droplet-transfer process enhanced the harvested amount compared with

that of U1, which had wires with the same wettability. Although these experiments were helpful to understand the phenomenon and to discuss ways for further enhancement, the setup with three wires was too small to characterize the fog-harvesting amount for practical use. The scaled-up fog harvester shown in Figure 2(c) was then used to evaluate harvesting performance. Figure 5 shows the results of fog harvesting by the scaled-up harvesters. In general, the harvested amount increased with increase in the fog velocity, similar to the result shown in Figure 3. The results from the multilayer setup show that the harvested amount increased with the number of stacked layers and yielded 15.99 g in 30 min for U3 at 2.0 m/s. This corresponds to 13.3% of the liquid contained in the fog stream. However, further increase was small when the number of wires was doubled or tripled. This was caused by the following two reasons. The first is the fog density at the location of each layer: because a portion of the fog droplets was already captured by upstream wires, the amount flowing in the layer on the downstream side simply decreased. The second reason is the flow velocity: owing to the pressure drop across the harvester, the velocity of incoming flow at latter layers decreased. This induced a low *St* number and low η_d, which means that the fog droplets avoided collision with the wires.

Figure 5 also shows the harvested amount for each layer. As an overall trend, the amount harvested at the first layer decreased with increase in number of layers, owing to droplet transfer from the hydrophobic wire in the second layer to the hydrophilic wire in first layer. In the present setup, the interlayer distance was set at 1 mm, as mentioned above. This may enhance inhibition of the fog

velocity and suppress the harvested amount compared with other experimental works that used a larger interlayer distance.[43,47] Furthermore, the amount harvested from the second layer increased with increase in number of layers. This could be attributed to droplet transfer from the third layer because the fog stream was no longer sufficient to initiate droplet motion along the stream.

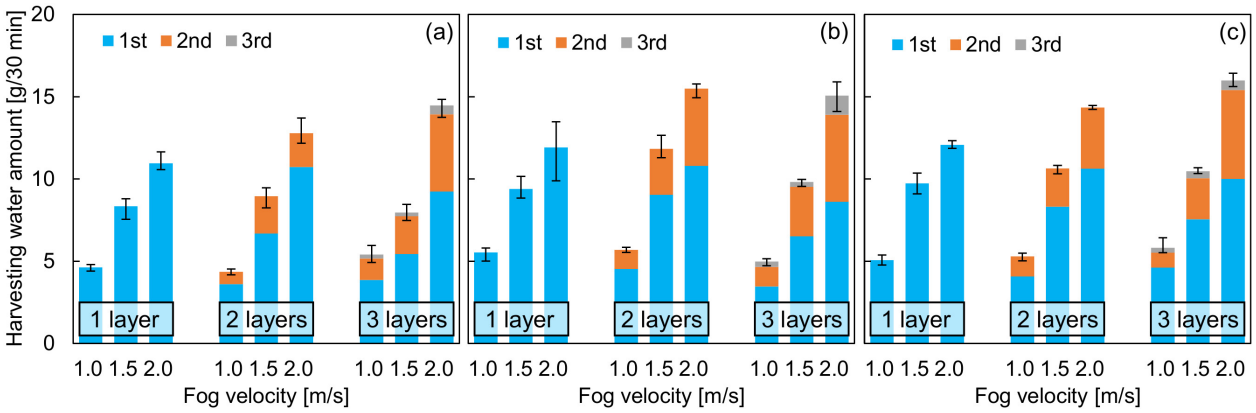

Figure 5 Amounts of fog harvested from scaled-up fog harvesters: (a) U1, (b) U2, and (c) U3

Although it is difficult to directly compare these results with those reported for other investigations because the fog density and velocity are different, performance of the fog harvester can be evaluated by comparing the normalized harvested amount. Here, we evaluated the fog-harvesting rate from our experimental results and conditions. Although the fog flow area was enlarged at the location of the harvester compared with the outlet of the fog stream (Figure 2(a)), the area where the fog stream collided was simply estimated as 25 mm × 25 mm. This leads to 0.0192 g/(mm^2·30 min) for a single layer and 0.0256 g/(mm^2·30 min) for three layers of U3 at a fog velocity of 2.0 m/s. These values are enhanced by 10% compared with those for U1, which were 0.0175 and 0.0231 g/(mm^2·30 min) for one and three layers, respectively. Table 2 shows the harvested

rate of recent fog-harvesting studies using harp, mesh, and other wire structures. Our results show relatively high water-harvesting rates although relatively thick wires were used. Droplet transfer between wires therefore plays an important role in enhancing the fog-harvesting efficiency. In addition, droplet transfer can help to reduce the occurrence of tangling of wires. Although the metal wires were of short length and relatively thick in the present study, thinner and longer wires made of

Table 2 Overview of results of fog-harvesting studies based on harps and meshes

No.	Shape	Material	Wire diameter	Fog velocity	Fog flow rate	Water harvesting rate	Ref.
1	Harp	Copper wire	400 μm	0.6 m/s	67±3 g/30 min	1.6 g/30 min at 10×20 mm	31
2	Harp	Steel wire	0.25 mm	0.15 m/s	141 g/h	~3g/(cm^2·h)	36
3	Harp	Stainless steel wire	0.254 mm	Less than 2 m/s	-	233 g/(m^2·min)	37
4	Harp (5 layers)	Polyethylene monofilaments	150~160 μm	4 m/s	-	~225 ml/(m^2·min)	43
5	Harp (4 layers)	PTFE filament with 3D bump surface	0.2 mm	-	350 g/h	287.6 ml/m^2/h	47
6	Web	Gel spindle-knot fiber coated with TPEE & chitosan fibers	100 μm	-	150 g/(m^2·s)	44.7 g/h at 4.91 cm^2	48
7	Fabric	Polyester yarns	-	0.5 m/s	300 ml/h	5424 mg/(cm^2·h)	49
8	Mesh	PMMA coated Aluminum	200 μm	0.3 m/s	250 g/h	4437.9 mg/(cm^2·h)	50
9	Janus mesh	Copper wire	40 μm	0.5 m/s	0.07 g/s	~2.2 g/(cm^2·h)	42
10	Janus mesh	Poly(lactic acid)	1 mm square	1.3 m/s	-	1.30 (g/cm^2·h)	41
11	Harp (1 layer)	Copper wire	0.5 mm	2.0 m/s	240 g/h	0.0192 g/(mm^2·30 min)	This work
12	Harp (3 layers)	Copper wire	0.5 mm	2.0 m/s	240 g/h	0.0256 g/(mm^2·30 min)	This work

a polymeric substance are reported to be potential materials for a practical fog harvester.[43,47–50] However, wires with those characteristics with uniform wettability showed tangling behavior.[37,39,51] This may not only degrade fog-harvesting performance, but also cause mechanical damage to the harvester; thus, droplet transportation between wires provides a way to avoid tangling during fog harvesting.

CONCLUSION

In this study, we investigated the effectiveness of droplet transfer between wires on fog-harvesting performance. A harvester comprising vertical wires was constructed and the effect of droplet-transfer process on the performance was assessed by varying the wire wettability and fog velocity. Although a low fog velocity was insufficient to initiate droplet transfer, transfer from an upstream hydrophobic wire to a downstream hydrophilic wire was observed at velocities above 1.5 m/s. The proportion of droplet transfer in the harvested amount exceeded 30% for the U3 experimental configuration, which enhanced fog-harvesting performance. A scaled-up harvester was developed and experiments were performed by stacking harvesters along the fog stream. The harvested amount increased with number of stacked layers, and the maximum harvesting efficiency reached 13.3% for U3. This result provides a new idea to enhance drainage of captured droplets and will help in designing a practical fog harvester to expand accessibility of fresh water.

Supporting Information

Brief descriptions of the additional movies (PDF)

Droplet removal process from unit U1 (Video S1) (AVI)

Droplet removal process from unit U3 (Video S2) (AVI)

AUTHOR INFORMATION

*Corresponding author

Yutaka Yamada

Tel.: +81 86 251 8046; E-mail: y.yamada@okayama-u.ac.jp

ORCID

Yutaka Yamada: 0000-0002-2823-6790

Kazuma Isobe: 0000-0002-8621-5015

Notes

The authors declare no competing financial interest.

ACKNOWLEDGMENTS

This work was partially supported by the Kurita Water and Environmental Foundation (Grant No.

21A044 and 22K014), Japan.

References

[1] Koncagül, E.; Conner, R. The United Nations World Water Development Report 2023: Partnerships and cooperation for water, 2023.

[2] Mekonnen, M. M.; A. Y. Hoekstra, A. Y. Four billion people facing severe water scarcity, Sci. Adv., 2016, 2, e1500323.

[3] Caldas, L.; Andaloro, A.; Calafiore, G.; Munechika, K.; Cabrini, S. Water harvesting from fog using building envelopes: part I, Water Environ. J, 2018, 32, 493-499.

[4] Alexandratos, S. D.; Barak, N.; Bauer, D.; Todd Davidson, F.; Gibney, B. R.; Hubbard, S. S.; Taft, H. L.; Westerhof, P. Sustaining Water Resources: Environmental and Economic Impact, ACS Sustainable Chem. Eng., 2019, 7, 2879-2888.

[5] Zhou, X.; Lu, H.; Zhao, F.; Yu, G. Atmospheric Water Harvesting: A Review of Material and Structural Designs, ACS Materials Lett., 2020, 2, 671-684.

[6] Seo, D.; Lee, J.; Lee, C.; Nam, Y. The effects of surface wettability on the fog and dew moisture harvesting performance on tubular surfaces, Sci. Rep., 2016, 6, 24276.

[7] Fessehaya, M.; Abdul-Wahab, S. A.; Savage, M. J.; Kohler, T.; Gherezghiher, T.; Hurni, H. Fog-water collection for community use, Renewable and Sustainable Energy Reviews, 2014, 29, 52-62.

[8] Ito, Y.; Chen, S.; Hirahara, R.; Konda, T.; Aoki, T.; Ueda, T.; Shimada, I.; Cannon, J. J.; Shao, C.;

Shiomi, J.; Tabata, K. V.; Noji, H.; Sato, K.; Aida, T. Ultrafast water permeation through nanochannels with a densely fluorous interior surface, Science, 2022, 376, 738-743.

[9] Lu, H.; Shi, W.; Guo, Y.; Guan, W.; Lei, C.; Yu, G. Materials Engineering for Atmospheric Water Harvesting: Progress and Perspectives, Adv. Mater., 2022, 34, 2110079

[10] Zhao, F.; Zhou, X.; Liu, Y.; Shi, Y.; Dai, Y.; Yu, G. Super Moisture-Absorbent Gels for All-Weather Atmospheric Water Harvesting, Adv. Mater, 2019, 31, 1806446.

[11] Mei, G.; Guo, Z. Special Wettability Materials Inspired by Multiorganisms for Fog Collection, Adv. Mater. Interfaces, 2022, 9, 2102484.

[12] Jiang, Y.; Machado, C.; Park, K.-C. K. From capture to transport: A review of engineered surfaces for fog collection, Droplet, 2023, e55.

[13] Azad, M. A. K.; Krause, T.; Danter, L.; Baars, A.; Koch, K.; Barthlott, W. Fog Collection on Polyethylene Terephthalate (PET) Fibers: Influence of Cross Section and Surface Structure, Langmuir, 2017, 33, 5555-5564.

[14] Malik, F. T.; Clement, R. M.; Gethin, D. T.; Krawszik, W.; Parker, A. R. Nature's moisture harvesters: a comparative review, Bioinspir. Biomim., 2014, 9, 031002.

[15] Yu, Z.; Zhu, T.; Zhang, J.; Ge, M.; Fu, S.; Lai, Y. Fog Harvesting Devices Inspired from Single to Multiple Creatures: Current Progress and Future Perspective, Adv. Funct. Mater., 2022, 32, 2200359.

[16] Parker, A. R.; Lawrence, C. R. Water Capture by a desert beetle, Nature, 2001, 414, 33-34.

[17] Zheng, Y.; Bai, H.; Huang, Z.; Tian, X.; Nie, F.-Q.; Zhao, Y.; Zhai, J.; Jiang, L. Directional water collection on wetted spider silk, Nature, 2010, 463, 640-643.

[18] Andrews, H. G.; Eccles, E. A.; Schofield, W. C. E.; Badyal, J. P. S. Three-Dimensional Hierarchical Structures for Fog Harvesting, Langmuir, 2011, 27, 3798-3802.

[19] Ju, J.; Bai, H.; Zheng, Y.; Zhao, T.; Fang, R.; Jiang, L. A multi-structural and multi-functional integrated fog collection system in cactus, Nat. Comm., 2012, 3, 1247.

[20] Comanns, P.; Effertz, C.; Hischen, F.; Staudt, K.; Böhme, W.; Baumgartner, W. Moisture harvesting and water transport through specialized micro-structures on the integument of lizards, Beilstein J. Nanotechnol., 2011, 2, 204-214.

[21] Gurera, D.; Bhushan, B. Multistep Wettability Gradient on Bioinspired Conical Surfaces for Water Collection from Fog, Langmuir, 2019, 35, 16944-16947.

[22] Zhang, K.; Chen, H.; Ran, T.; Zhang, L.; Zhang, Y.; Chen, D.; Wang, Y.; Guo, Y.; Liu, G. High-Efficient Fog Harvest from a Synergistic Effect of Coupling Hierarchical Structures, ACS. Appl. Mater. Interfaces, 2022, 14, 33993-34001.

[23] Tian, Y.; Zhu, P.; Tang, X.; Zhou, C.; Wang, J.; Kong, T.; Xu, M.; Wang, L. Large-scale water collection of bioinspired cavity-microfibers, Nat. Comm., 2017, 8, 1080.

[24] An, Q.; Wang, J.; Zhao, F.; Wang, L. Fog collection on a superhydrophobic/hydrophilic composite spine surface, RSC Advances, 2020, 10, 9318-9323.

[25] Song, Y.-Y.; Yu, Z.-P.; Dong, L.-M.; Zhu, M.-L.; Ye, Z.-C.; Shi, Y.-J.; Liu, Y. Cactus-Inspired

Janus Membrane with a Conical Array of Wettability Gradient for Efficient Fog Collection, Langmuir, 2021, 37, 13703-13711.

[26] Ju, J.; Xiao, K.; Yao, X.; Bai, H.; Jiang, L. Bioinspired Conical Copper Wire with Gradient Wettability for Continuous and Efficient Fog Collection, Adv. Mater., 2013, 25, 5937-5942.

[27] Lin, J.; Tan, X.; Shi, T.; Tang, Z.; Liao, G. Leaf Vein-Inspired Hierarchical Wedge-Shaped Tracks on Flexible Substrate for Enhanced Directional Water Collection, ACS Appl. Mater. Interfaces, 2018, 10, 44815-44824.

[28] Wang, M.; Liu, Q.; Zhang, H.; Wang, C.; Wang, L.; Xiang, B.; Fan, Y.; Guo, C. F.; Ruan, S. Laser Direct Writing of Tree-Shaped Hierarchical Cones on a Superhydrophobic Film for High-Efficiency Water Collection, ACS Appl. Mater. Interfaces, 2017, 9, 29248-29254.

[29] Kostal, E.; Stroj, S.; Kasemann, S.; Matylitsky, V.; Domke, M. Fabrication of Biomimetic Fog-Collecting Superhydrophilic-Superhydrophobic Surface Micropatterns Using Femtosecond Lasers, Langmuir, 2018, 34, 2933-2941.

[30] Bai, H.; Wang, L.; Ju, J.; Sum, R.; Zheng, Y.; Jiang, L. Efficient Water Collection on Integrative Bioinspired Surfaces with Star-Shaped Wettability Patterns, Adv. Mater., 2014, 26, 5025-5030.

[31] Zhong, L.; Zhang, R.; Li, J.; Guo, Z.; Zeng, H. Efficient Fog Harvesting Based on 1D Copper Wire Inspired by the Plant Pitaya, Langmuir, 2018, 34, 15259-15267.

[32] Bai, H.; Wang, X.; Li Z.; Wen, H.; Yang, Y.; Li, M.; Cao, M. Improved Liquid Collection on a Dual-Asymmetric Superhydrophilic Origami, Adv. Mater., 2023, 35, 2211596.

[33] Park, J.; Lee, C.; Lee, S.; Cho, H.; Moon, M.-W.; Kim, S. J. Clogged water bridges for fog harvesting, Soft Matter, 2021, 17, 136-144.

[34] Park, K.-C.; Chhatre, S. S.; Srinivasan, S.; Cohen, R. E.; McKinley, G. H. Optimal Design of Permeable Fiber Network Structures for Fog Harvesting, Langmuir, 2013, 29, 13269-13277.

[35] Goswami, S.; Sidhpuria, R. M.; Khandekar, S. Effect of Droplet-Laden Fibers on Aerodynamics of Fog Collection on Vertical Fiber Arrays, Langmuir, 2023, 39, 18238-18251.

[36] Shi, W.; Anderson, M. J.; Tulkoff, J. B.; Kennedy, B. S.; Boreyko, J. B. Fog Harvesting with Harps, ACS Appl. Mater. Interfaces, 2018, 10, 11979-11986.

[37] Shi, W.; De Koninck, L. H.; Hart, B. J.; Kowalski, N. G.; Fugaro, A. P.; van der Sloot, T. W.; Ott, R. S.; Kennedy, B. S.; Boreyko, J. B. Harps under Heavy Fog Conditions: Superior to Meshes but Prone to Tangling, ACS Appl. Mater. Interfaces, 2020, 12, 48124-48132.

[38] Kaindu, J. K.; Murphy, K. R.; Kowalski, N. G.; Jones, A. N.; Fleming, M. D.; Kennedy, B. S.; Boreyko, J. B. Antitangling and manufacturable Fog Harps for high-efficiency water harvesting, Droplet, 2023, 2, e78.

[39] Duprat, C.; Protière, S.; Beebe, A. Y.; Stone, H. A. Wetting of flexible fibre arrays, Nature, 2012, 482, 510-513.

[40] Liu, C.; Lu, C.; Zhan, H.; Ge, W.; Feng, S.; Liu, Y. Multibioinspired JANUS Membranes with Spatial Surface Refreshment for Enhanced Fog Collection, Adv. Mater. Interfaces, 2021, 8, 2101212.

[41] Lee, J. H.; Lee, Y. J.; Kim, H.-Y.; Moon, M.-W.; Kim, S. J. Unclogged Janus Mesh for Fog

Harvesting, ACS Appl. Mater. Interfaces, 2022, 14, 21713-21726.

[42] Zhong, L.; Feng, J.; Guo, Z. An alternating nanoscale (hydrophilic-hydrophobic)/hydrophilic Janus cooperative copper mesh fabricated by a simple liquidus modification for efficient fog harvesting, J. Mater. Chem. A, 2019, 7, 8405-8413.

[43] Azeem, M.; Guérin, A.; Dumais, T.; Caminos, L.; Goldstein, R. E.; Pesci, A. I.; de Dios Rivera, J.; Josefina Torres, M.; Wiener, J.; Luis Campos, J.; Dumais, J. Optimal Design of Multilayer Fog Collectors, ACS Appl. Mater. Interfaces, 2020, 12, 7736-7743.

[44] de Dios Rivera, J. Aerodynamic collection efficiency of fog water collectors, Atmos. Res., 2011, 102, 335-342.

[45] Mukhopadhyay, A.; Datta, A.; Dutta, P. S.; Datta, A.; Ganguly R. Droplet Morphology-Based Wettability Tuning and Design of Fog Harvesting Mesh to Minimize Mesh-Clogging, Langmuir, 2024, 40, 8094-8107

[46] Yamada, Y.; Sakata, E.; Isobe, K.; Horibe, A. Wettability Difference Induced Out-of-Plane Unidirectional Droplet Transport for Efficient Fog Harvesting, ACS Appl. Mater. Interfaces, 2021, 13, 35079-35085.

[47] Nguyen, L. T.; Bai, Z.; Zhu, J.; Gao, C.; Liu, X.; Wagaye, B. T.; Li, J.; Zhang, B.; Guo, J. Three-Dimensional Multilayer Vertical Filament Meshes for Enhancing Efficiency in Fog Water Harvesting, ACS Omega, 2021, 6, 3910-3920.

[48] Liu, Y.; Yang, N.; Gao, C.; Li, X.; Guo, Z.; Hou, Y.; Zheng, Y. Bioinspired Nanofibril-Humped

Fibers with Strong Capillary Channels for Fog Capture, ACS Appl. Mater. Interfaces, 2020, 12, 28876-28884.

[49] Yu, Z.; Li, S.; Liu, M.; Zhu, R.; Yu, M.; Dong, X.; Sun, Y.; Fu, S. A dual-biomimetic knitted fabric with a manipulable structure and wettability for highly efficient fog harvesting, J. Mater. Chem. A, 2022, 10, 304-312.

[50] El-Maghraby, H. F.; Alhumaidi, A.; Alnaqbi, M. A.; Sherif, M.; Tai, Y.; Hassan, F.; Greish, Y. E. Bioinspired Asymmetric Surface Property of Functionalized Mesh to Maximize the Efficiency of Fog Harvesting, ChemNanoMat, 2022, 8, e202200327.

[51] Shi, W.; van der Sloot, T. W.; Hart, B. J.; Kennedy, B. S.; Boreyko, J. B. Harps Enable Water Harvesting under Light Fog Conditions, Adv. Sustainable Syst., 2020, 4, 2000040.

1 TOC graphic

2 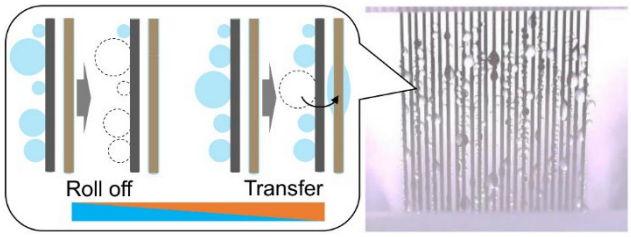

3